

Australian Journal of Mechanical Engineering

ISSN: (Print) (Online) Journal homepage: www.tandfonline.com/journals/tmec20

Robust control and performance evaluation of slow and fully active electromechanical suspension systems

İ. Sina Kuseyri

To cite this article: İ. Sina Kuseyri (24 Mar 2025): Robust control and performance evaluation of slow and fully active electromechanical suspension systems, Australian Journal of Mechanical Engineering, DOI: 10.1080/14484846.2025.2478676

To link to this article: https://doi.org/10.1080/14484846.2025.2478676

Published online: 24 Mar 2025.

Submit your article to this journal

View related articles

View Crossmark data

Full Terms & Conditions of access and use can be found at
https://www.tandfonline.com/action/journalInformation?journalCode=tmec20

AUSTRALIAN JOURNAL OF MECHANICAL ENGINEERING
https://doi.org/10.1080/14484846.2025.2478676

Taylor & Francis
Taylor & Francis Group

Check for updates

Robust control and performance evaluation of slow and fully active electromechanical suspension systems

İ. Sina Kuseyri

Faculty Department of Mechanical Engineering Maltepe, Marmara University Engineering, İstanbul, Turkey

ABSTRACT

The objective of this paper is to design and compare the performance of robust H_∞ controllers for slow and fully active electromechanical suspension systems. H_∞ controllers are synthesised based on half-car model dynamics. The criteria used for comparison are linear and angular body accelerations representing the ride comfort, tire compressions for handling, and actuator effort for energy consumption. It is shown that slow-active electromechanical suspension systems consume considerably less control energy relative to fully active electromechanical suspension systems, albeit with a slight decrease in performance.

ARTICLE HISTORY
Received 4 February 2024
Accepted 5 March 2025

KEYWORDS
Robust control; slow-active suspension; fully active suspension; suspension performance

1. Introduction

The primary function of the suspension system is to isolate the vehicle body from shock loads and vibration due to disturbances in the road surface and it must accomplish this without impairing the steering and handling performance of the vehicle. To ensure passenger comfort, the suspension system must provide a high degree of isolation for the vehicle body from the loads due to disturbances from the road, tyre irregularities, and wheel out-of-balance forces. Moreover, it must keep the wheels in close contact with the road surface to ensure adequate road holding when braking, accelerating or cornering. These functions must then be optimised within several constraints such as the relative body/wheel workspace usage and vehicle attitude control in manoeuvring. In fact, the conflict between these various optimisation objectives is the main problem in the suspension system design. Riding comfort requires an optimal damping setting, which helps to decrease the acceleration of the vehicle body. Handling performance depends on good road-holding capacity, which is proportional to tire compression. These performance requirements motivate the implementation of active suspension systems and associated control system design to replace the conventional passive systems.

Research on active suspension systems has commenced in 1970s, using mainly the standard quarter car suspension model (Dahlberg 1978; Eckert 1973). PID, LQ, and Skyhook control design techniques and their combinations are the primary methods in active suspension system design. In (Michelberg, Palkovics, and Bokor 1993), authors use a quarter car model to show the disadvantage of LQG control in terms of robustness. It has been shown that if the parameters of the system differ from their nominal values, the performance of the controlled system degrades. In (De Jager 1991) author compares several types of LQ controllers on a quarter car model. Linear Quadratic Regulator (LQR) controllers are found to be more robust over Linear Quadratic Gaussian (LQG) or Linear Quadratic Output Feedback (LGOF) controllers. However, due to the large number of sensors required, the LQR controller was not considered to be practical. In (Hrovat 1997) the author discusses various models for controller synthesis. Using an LQ controller with suspension travel and vertical vehicle speed as state variables, he concludes that the closed-loop system functions as a 'skyhook damper'. The author argues that a real 'skyhook' is physically not possible and better performance can be achieved when the active device emulates a damper connected to a smooth inertial ground. He also evaluates the effectiveness of the preview and proves the effectiveness with numerical results. Author also discusses the robust stability of LQG controllers, and he arrives at the conclusion of Doyle (1978), that is, no guaranteed margins exist. In (Yamashita et al. 1994) authors implement robust control to mitigate vertical acceleration and to improve handling using a full car model. A multiplicative uncertainty is introduced to account for varying body mass and actuator uncertainty. Nominal and robust H_∞ controllers designed are compared with the passive case. It has been shown that active systems incorporating either nominal or robust controllers have superior performance over the passive system. In (Sharkawy 2005) Fuzzy control has been applied. Its performance is better than standard LQR control,

CONTACT İ. Sina Kuseyri sina.kuseyri@marmara.edu.tr
© 2025 Engineers Australia

however finding the output surface required by fuzzy control is developed using Lyapunov direct method. However, the stability of the closed-loop system is not shown to be ensured in the paper.

In (Lauwerys, Swevers, and Sas 2005) robust controller design using a hydraulic actuator is verified experimentally. The dynamics of the quarter car test setup are identified using a frequency domain approach in which the parameters and uncertainties of the model are estimated from measurements. The controller design is aimed at reducing the vehicle body vibrations at human sensitive vibration comfort range without amplifying the body acceleration or tire force in other frequency regions. The performance increase in suppression of the vibration in human sensitive comfort range increased two folds without serious drawbacks in dynamic tire load variations. Another experimental test setup was built in (Lee and Kim 2010) using an electromechanical actuator. The road excitations considered are based on a fixed shape road profile. Accelerations of the sprung and unsprung mass and the suspension travel are measured. Using these measurements, the performance of a lead-lag, a fuzzy, and an LQ controller is discussed. Performance of the LQ controller did not match the other two controllers due to the errors in the state estimation.

The research in Hamersma and Els 2015 consists of comparison of suspension system model outputs with the measurement data from sensors mounted on a real car. Three models and their respective measurement data are compared: full-car, half-car, and quarter-car models. The closest results between simulations and measurement data belong to the full-car model. Half-car model simulation results can also be considered close to the measurement results, but the quarter-car simulation results are comparatively distant from the actual measurements.

In this study, the half-car model is used rather than the generally used quarter-car model to incorporate more degrees of freedom, specifically the angular motion of the vehicle, to reduce the error between model and reality as shown in (Hamersma and Els 2015). Furthermore, since a car always has variations in its parameters, our active suspension design will be based on robust control. The well-known active electromechanical active suspension system (Gysen et al. 2008) which is also called fully active suspension system suffers the major problem of high power consumption. However, it is shown in our work that the slow-active electromechanical suspension system (El Madany, Bassam, and Fayed 2011) relaxes the high power consumption requirement of active suspension systems, incorporating an extra built-in spring in series with the actuator. Based on the mathematical models developed, we compare the performance of slow and fully active electromechanical suspension systems with respect to their driving comfort, road handling, and the actuator effort.

2. Active electromechanical suspension models

The main components of the passive suspension systems are the spring and damper elements. In active systems, an actuator is used either instead of these passive elements or it may be mounted in parallel or in series with them. In modelling these systems a half-car model can be used with four degrees of freedom containing pitch and bounce information. Schematic representations of slow and fully active suspension models are given in Figure 1.

Both systems have three rigid bodies which are the vehicle body, front, and rear wheel assemblies. We make the following assumptions in the derivation of the equations governing the dynamics of the suspension models:

- Wheel assemblies enable movement only in the vertical direction.
- The stiffness of tires and the stiffness and damping of the suspensions can be represented by linear elements.
- The suspension system applies force point contacts through the vehicle body.
- The vehicle horizontally travels at a constant speed.

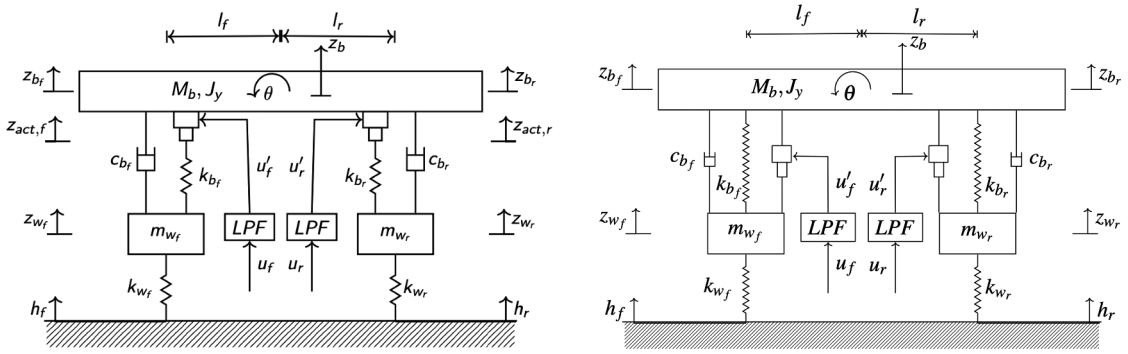

Figure 1. Slow (left) and fully active (right) half car suspension models.

2.1. Slow-active model

In slow-active systems, an actuator is installed in series with a passive spring (El Madany, Bassam, and Fayed 2011). A passive damper would typically be used in parallel with the spring or between the body and wheel of the vehicle or in conjunction with the system. The actuator may be used to introduce energy in or out of the system over a certain limited bandwidth. Slow actuators are usually comprised of an electric motor with a mechanical rotary to linear motion transformer. They have a relatively limited bandwidth. Therefore, they have the practical advantage of lower cost over the fast linear motors used in fully active systems. In the mathematical model of slow-active systems, a second order low pass filter is used imposing an idealised frequency limitation to enable the investigation of various cut-off frequencies. A generic form of second order low-pass filter can be defined by its input/output equation $\ddot{y} + 2\zeta\omega_{0,act}\dot{y} + \omega_{0,act}^2 y = \omega_{0,act}^2 u$. The control law is based on a displacement demand signal which is a function of some or all states of the suspension system.

The dynamic equations of the car body for bounce and pitch motions are

$$M_b \ddot{z}_b = -F_f - F_r, \tag{2.1a}$$

$$J_y \ddot{\theta} = l_f F_f - l_r F_r. \tag{2.1b}$$

Vertical dynamics of the tyres are

$$m_{w_f} \ddot{z}_{w_f} = F_f - F_{w_f}, \tag{2.2a}$$

$$m_{w_r} \ddot{z}_{w_r} = F_r - F_{w_r}. \tag{2.2b}$$

In equations (2.1) and (2.2), the forces provided by the springs, dampers and the actuators are

$$F_f = k_{b_f}(z_{act,f} - z_{w_f}) + c_{b_f}(\dot{z}_{b_f} - \dot{z}_{w_f}), \tag{2.3a}$$

$$F_r = k_{b_r}(z_{act,r} - z_{w_r}) + c_{b_r}(\dot{z}_{b_r} - \dot{z}_{w_r}), \tag{2.3b}$$

$$F_{w_f} = k_{w_f}(z_{w_f} - h_f), \tag{2.3c}$$

$$F_{w_r} = k_{w_r}(z_{w_r} - h_r). \tag{2.3d}$$

The displacements at the front and rear tyre locations are $z_{b_f} = z_b - l_f\theta$, and $z_{b_r} = z_b + l_r\theta$ respectively.

Substituting these forces in equations (2.3) into the equations (2.1) and (2.2), the equations of motion for the four degrees of freedom are

$$\ddot{\theta} = \frac{1}{J_y}[(-l_f{}^2 c_{b_f} - l_r{}^2 c_{b_r})\dot{\theta} + (l_f c_{b_f} - l_r c_{b_r})\dot{z}_b - l_f k_{b_f} z_{w_f} - l_f c_{w_f}\dot{z}_{w_f} + l_r k_{b_r} z_{b_r} + l_r c_{b_r}\dot{z}_{w_r} + l_f k_{b_f} z_{act,f} - l_r k_{b_r} z_{act,r}], \tag{2.4a}$$

$$\ddot{z}_b = \frac{1}{M_b}[(l_f c_{b_f} - l_r c_{b_r})\dot{\theta} - (c_{b_f} + c_{b_r})\dot{z}_b + k_{b_f} z_{w_f} + c_{b_f}\dot{z}_{w_f} + k_{b_r} z_{w_r} + c_{b_r}\dot{z}_{w_r} - k_{b_f} z_{act,f} - kb_r z_{act,r}], \tag{2.4b}$$

$$\ddot{z}_{w_f} = \frac{1}{m_{w_f}}[-l_f c_{b_f}\dot{\theta} + c_{b_f}\dot{z}_b - (k_{b_f} + k_{w_f}) z_{w_f} - c_{b_f}\dot{z}^{w_f} + k_{b_f} z_{act,f} + k_{w_f} h_f], \tag{2.4c}$$

$$\ddot{z}_{w_r} = \frac{1}{m_{w_r}}[l_r c_{b_r}\dot{\theta} + c_{b_r}\dot{z}_b - (k_{b_r} + k_{w_r}) z_{w_r} - c_{b_r}\dot{z}_{w_r} + k_{b_r} z_{act,r} + k_{w_r} h_r]. \tag{2.4d}$$

Second-order low pass filter dynamics for both the front and rear actuators is

$$\ddot{u}'_{f,r} + 2\zeta\omega_{0,act_{f,r}}\dot{u}'_{f,r} + \omega_{0,act_{f,r}}^2 u'_{f,r} = \omega_{0,act_{f,r}}^2 u_{f,r}. \tag{2.5}$$

Here the actuator inputs u'_f and u'_r are

$$u'_f = z_{b_f} - z_{act,f} = z_b + l_f\theta - z_{act,f}, \tag{2.6a}$$

$$u'_r = z_{b_r} - z_{act,r} = z_b - l_r\theta - z_{act,r}. \tag{2.6b}$$

Differentiating twice the equations (2.6) and using the previous results leads to the actuators' dynamics

$$\ddot{z}_{act,f} = -l_f w_{0,act_f}^2\theta + (-2l_f w_{0,act_f} + l_f c_{b_f} a_1 - l_r c_{b_r} a_2)\dot{\theta} + w_{0,act_f}^2 z_b + (2\zeta w_{0,act_f} - c_{b_f} a_1 - c_{b_r} a_2)\dot{z}_b + k_{b_f} a_1 z_{b_f} + c_{b_f} a_1 \dot{z}_{b_f} + k_{b_r} a_2 z_{b_r} + c_{b_r} a_2 \dot{z}_{b_r} - (w_{0,act_f}^2 + k_{b_f} a_1) z_{act,f} - 2\zeta w_{0,act_f}\dot{z}_{act,f} - k_{b_r} a_2 z_{act,r} - w_{0,act_f}^2 u_f, \tag{2.7a}$$

$$\ddot{z}_{act,r} = l_r w_{0,act_f}^2\theta + (2l_r w_{0,act_r} + l_f c_{b_f} a_2 - l_r c_{b_r} a_3)\dot{\theta} + w_{0,act_r}^2 z_b + (2\zeta w_{0,act_r} - c_{b_f} a_2 - c_{b_r} a_3)\dot{z}_b + k_{b_f} a_2 z_{b_f} + c_{b_f} a_2 \dot{z}_{b_f} + k_{b_r} a_3 z_{b_r} + c_{b_r} a_3 \dot{z}_{b_r} - k_{b_f} a_2 z_{act,f} - (w_{0,act_r}^2 + k_{b_r} a_3) z_{act,r} - 2\zeta w_{0,act_r}\dot{z}_{act,r} - w_{0,act_r}^2 u_r. \tag{2.7b}$$

where $a_1 = 1/M_b + l_f^2/J_y$, $a_2 = 1/M_b - l_f l_r/J_y$, and $a_3 = 1/M_b + l_r^2/J_y$.

2.2. Fully active model

Fully active systems use an actuator in parallel with a damper and a spring (Koch 2010). Actuator is a linear motor with relatively high bandwidth. The nominal actuator dynamics can be represented by a first-order transfer function to reflect the larger gain at high frequencies. A generic form of a first-order low-pass filter can be defined by its input/output equation $\tau \dot{y} + y = bu$. The control law of the limited actuator is again based on a displacement demand signal which is a function of some or all the state variables of the system.

Similar to the slow-active system, considering the forces acting on the three masses, the equations of motion for the four degrees of freedom are

$$\begin{aligned}\ddot{\theta} = \frac{1}{J_y}[&(l_f c_{b_f} - l_r c_{b_r})\dot{z}_b \\ &- (l_f^2 c_{b_f} + l_r^2 c_{b_r})\,\dot{\theta} + l_f k_{b_f}(z_{b_f} - z_{w_f}) - l_f c_{b_f}\dot{z}_{w_f} \\ &- l_r k_{b_r}(z_{b_r} - z_{w_r}) + l_r c_{b_r}\dot{z}_{w_r} - l_f u'_f + l_r u'_r],\end{aligned} \tag{2.8a}$$

$$\begin{aligned}\ddot{z}_b = \frac{1}{M_b}[&-(c_{b_f} + c_{b_r})\dot{z}_b \\ &+ (l_f c_{b_f} - l_r c_{b_r})\,\dot{\theta} - k_{b_f}(z_{b_f} - z_{w_f}) + c_{b_f}\dot{z}_{w_f} \\ &- k_{b_r}(z_{b_r} - z_{w_r}) + c_{b_r}\dot{z}_{w_r} + u'_f + u'_r],\end{aligned} \tag{2.8b}$$

$$\begin{aligned}\ddot{z}_{w_f} = \frac{1}{m_{w_f}}[&-k_{w_f} z_b + c_{b_f}\dot{z}_b + l_f k_{w_f}\theta \\ &- l_f c_{b_f}\,\dot{\theta} + (k_{b_f} + k_{w_f})(z_{b_f} - z_{w_f}) - c_{b_f}\dot{z}_{w_f} \\ &+ k_{w_f} h_f - u'_f],\end{aligned} \tag{2.8c}$$

$$\begin{aligned}\ddot{z}_{w_r} = \frac{1}{m_{w_r}}[&-k_{w_r} z_b + c_{b_r}\dot{z}_b - l_r k_{w_r}\theta \\ &+ l_r c_{b_r}\,\dot{\theta} + (k_{b_r} + k_{w_r})(z_{b_r} - z_{w_r}) - c_{b_r}\dot{z}_{w_r} \\ &+ k_{w_r} h_r - u'_r].\end{aligned} \tag{2.8d}$$

First-order low pass filter dynamics for both the front and rear actuators is

$$\tau\,\ddot{u}'_{f,r} + u'_{f,r} = bu_{f,r}. \tag{2.9}$$

2.3. Models in state-space

Models derived in previous sections can be represented in state-space for further controller synthesis in the form

$$\ddot{x} = Ax + B_1 w + B_2 u \tag{2.10a}$$

$$z = C_1 x + D_{11} w + D_{12} u \tag{2.10b}$$

$$y = C_2 x + D_{21} w + D_{22} u \tag{2.10c}$$

State vectors for the slow and fully active systems' equations (2.10) are chosen, respectively, to be

$$x_{sa} = [\,\theta \quad \theta \quad z_b \quad z_b \quad z_{w_f} \quad z_{w_f} \quad z_{w_r} \quad z_{w_r} \quad z_{act,f} \quad z_{act,f}\; z_{act,r} \quad z_{act,r}\,]^T,$$

$$x_{fa} = [\,\theta \quad \theta \quad z_b \quad z_b \quad z_{b_f} - z_{w_f} \quad z_{w_f} \quad z_{b_r} - z_{w_r} \quad z_{w_r} \quad u'_f \quad u'_r\,]^T.$$

Disturbance and input vectors of both systems are comprised of road front/rear deflections and front/rear control inputs, i.e. $w = [h_f \quad h_r]^T$, $u = [u_f \quad u_r]^T$.

The performance outputs of the systems are front and rear tire compressions, body translational and rotational accelerations, front suspension and rear suspension travels, and front and rear actuator efforts. Measurements are body translational and rotational accelerations, front and rear tire accelerations, and the front and rear suspension travels, i.e. $z = [z_{w_f} - h_f \; z_{w_r} - h_r \; \ddot{z}_b \; \ddot{\theta} \; z_{b_f} - z_{w_f} \; z_{b_r} - z_{w_r} \; u_f \; u_r]^T$, and $y = [\ddot{z}_b \; \ddot{\theta} \; \ddot{z}_{w_f} \; \ddot{z}_{w_r} \; z_{b_f} - z_{w_f} \; z_{b_r} - z_{w_r}]^T$.

Matrices in the state-space representation (2.10) can be easily derived for the slow and fully active systems using the equations of motion given in the preceding subsections.

3. Controller synthesis

One approach in modelling for controller synthesis is to arrange the open-loop system in LFT (linear fractional transformation) form.

$$\begin{pmatrix} z \\ y \end{pmatrix} = P(s)\begin{pmatrix} w \\ u \end{pmatrix} = \begin{pmatrix} P_{11}(s) & P_{12}(s) \\ P_{21}(s) & P_{22}(s) \end{pmatrix}\begin{pmatrix} w \\ u \end{pmatrix}$$

$$u = K(s)y$$

The closed-loop system N can then be described in a lower LFT form, where $N = P_{11} + P_{12}K(I - P_{22}K)^{-1}P_{21}$. Control objective is to minimise the H_∞ norm of the closed-loop system N from w to z. The H_∞ norm of the closed-loop system is defined as $\| N\|_\infty := \sup_{\omega\in}\bar{\sigma}(N(j\omega))$, where $\bar{\sigma}$ denotes the maximum singular value. Components of the generalised plant P can be obtained from the state-space representation of the active suspension system incorporating the weights required for performance optimisation.

Weights used in the controller synthesis are chosen from previous literature on active suspension system design. The sprung mass (car body) acceleration weights are generated based on ISO2631–1 standard reflecting the sensitivity of passengers to road-induced vibrations. We use the fifth-order transfer function adapted from (Zuo and Nayfeh 2003).

$$W_{\ddot{z}_b}(s) = \frac{87.72s^4 + 1138s^3 + 11336s^2 + 5453s + 5509}{s^5 + 92.69s^4 + 2550s^3 + 25969s^2 + 81057s + 79783}$$

The tire compression weights used are from (Pacejka and Besselink 1997).

$$W_{z_w}(s) = \frac{\frac{1}{2\pi 12}s + 1}{\frac{1}{2\pi 0.6}s + 1}$$

The smooth road conditions are defined by the weights

$$W_{r_{f,r}}(s) = \frac{1}{s+6}$$

which are used to shape the white noise disturbance inputs.

Due to the fact that tire and chassis resonances can occur over 30 hz, it is decided to limit the actuator effort above this frequency using a second order high-pass filter in accordance with (Gysen et al. 2008).

$$W_u(s) = \frac{\frac{1}{(2\pi 30)^2}s^2 + \frac{\sqrt{2}}{(2\pi 30)}s + 1}{\frac{1}{(2\pi 200)^2}s^2 + \frac{\sqrt{2}}{(2\pi 200)}s + 1}$$

We have also considered the uncertainties in our suspension system models, and we have incorporated parametric and dynamic uncertainties (unmodeled dynamics) in our controller design. Robust controller synthesis is implemented using the structured uncertainty block Δ, comprised of parametric and dynamic uncertainties, as shown in Figure 2. Weights used for the dynamic uncertainty

$$W_{dyn} = \frac{\frac{1}{(2\pi 30)^2}s^2 + \frac{1.414}{2\pi 30} + 1}{\frac{1}{(2\pi 400)^2}s^2 + \frac{1.414}{2\pi 400} + 1}$$

and the parametric uncertainties (Table 1) are based on (Van der Sande et al. 2013).

4. Numerical simulations

4.1. Road conditions and vehicle parameters

Simulations are made using stochastic and deterministic road disturbances. For stochastic disturbance models, representing smooth and rough road conditions, a first-order filter with white noise input can be used. Road condition parameters are given in Table 2.

$$\frac{1}{vV_x}\dot{h} + h = w$$

Here h is the vertical road heave, V_x is the vehicle's horizontal speed, and w is the white noise signal. Parameter v represents the cut-off frequency. The computed heave value is multiplied by the gain ψ given in the following table. t_s is the sampling time and is defined to be 0.0025 s (Liu et al. 2013).

The deterministic disturbance, specifically the bumpy road condition, is defined to be $h = 0.015(1 - cos(8\pi t))$ which specifes a maximum bump height of 0.3 m (Pacejka and Besselink 1997). Our suspension systems are based on a half-car vehicle model. Hence, a delay on the time of application of road disturbances must be introduced in the simulations. The delay which depends on the wheel base and horizontal speed of the vehicle is $t_d = (l_r - l_f)/V_x$.

Figure 3 depicts sample road disturbance signals in the time domain.

Vehicle parameters used in the simulations are given in Table 3 (Michelberger, Palkovics, and Bokor 1993).

4.2. Simulation outcomes

Vehicle response to disturbances considering the vertical and angular accelerations of the sprung mass with passive suspensions are shown in Figure 4. Figures on the left are for linear accelerations, whereas the figures on the right are for angular accelerations. RMS and maximum PSD accelerations of the vehicle with passive suspensions on test road conditions are given in Table 4.

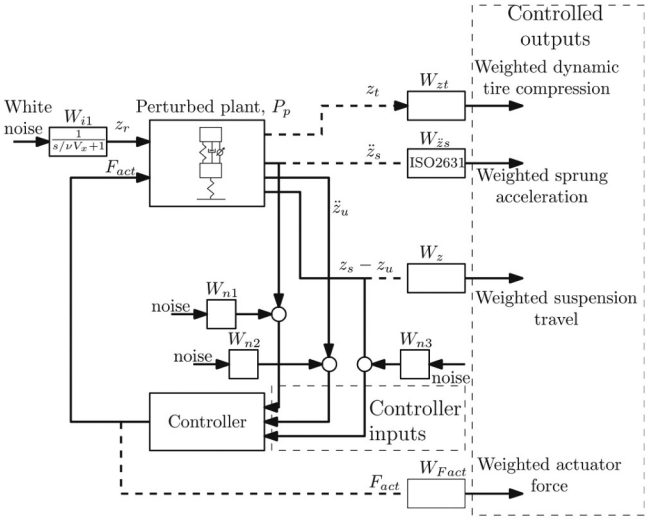

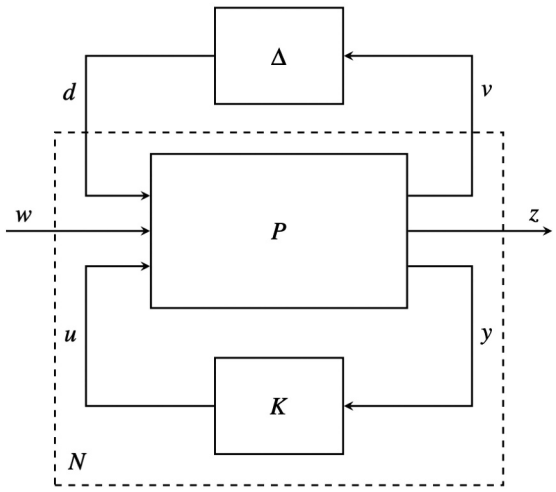

Figure 2. Robust control structure.

Table 1. Uncertainty parameters of the half car model.

Parameter name	Mean value	Deviation
Sprung mass	997 kg	−85/+150 kg
Tire stiffness	234 kN/m	±30 kN/m
Front damping coefficient	3500 N.s/m	−550/+250 N.s/m
Rear damping coefficient	2800 N.s/m	−550/+250 N.s/m

Table 2. Road condition parameters.

Road type	v (rad/m)	V_x (m/s)	ψ
Smooth	0.2	30	$0.05\sqrt{\frac{0.001}{t_s}}$
Rough	0.8	7.5	$0.125\sqrt{\frac{0.001}{t_s}}$

Active suspension systems are designed with controllers synthesised using the Robust Control Toolbox of Matlab. During the simulations for active suspensions, we have assumed that the RMS values of sensor measurement errors for vertical acceleration, angular acceleration, and suspension travel are $\pm 0.024\ \text{m/s}^2$, $\pm 0.078\ \text{rad/s}^2$, and ± 0.002 m, respectively (Li 2012).

Vehicle response to smooth road conditions with active suspensions considering the vertical and angular accelerations of the sprung mass and the required actuator efforts (front) are shown in Figure 5.

PSD plots for the body linear and angular accelerations are shown in Figure 6. Plot on the left is for linear acceleration, whereas the plot on the right is for angular acceleration.

Similarly, vehicle response to rough road conditions with active suspensions considering the vertical and angular accelerations of the sprung mass and the required actuator efforts are shown in Figure 7.

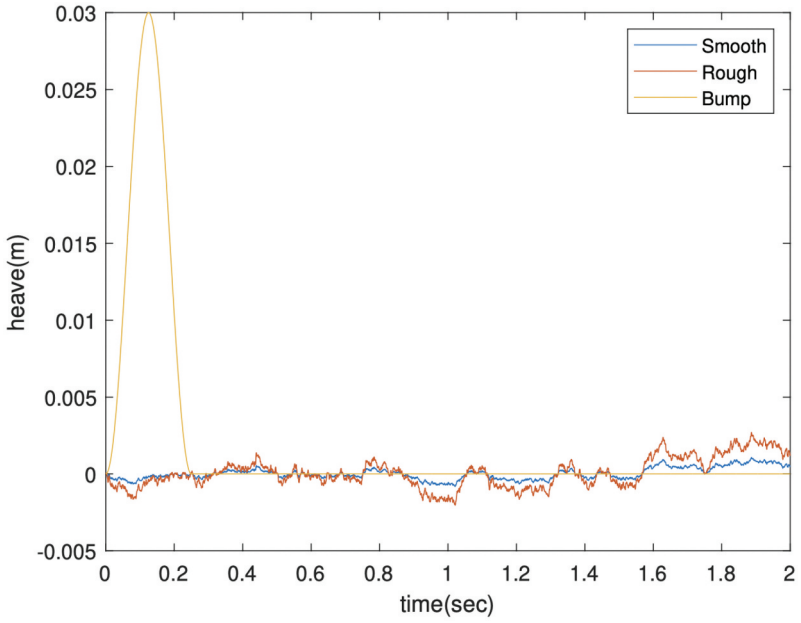

Figure 3. Road disturbance.

Table 3. Vehicle parameters.

Parameters	Symbol	Value
Half car mass (kg)	M_b	997
Front wheel mass (kg)	m_{w_f}	40
Rear wheel mass (kg)	m_{w_r}	40
Front wheel base (m)	l_f	1.30
Rear wheel base (m)	l_r	1.65
Front suspension spring stiffness (kN/m)	k_{b_f}	111
Rear suspension spring stiffness (kN/m)	k_{b_r}	67
Front suspension damping coefficient (kN.s/m)	c_{b_f}	3.5
Rear suspension damping coefficient (kN.s/m)	c_{b_r}	2.8
Front tire stiffness (kN/m)	k_{w_f}	234
Rear tire stiffness (kN/m)	k_{w_r}	234
Car pitch moment of inertia (kg.m^2)	J_y	3800
Slow-active actuators' natural frequency (rad/s)	$w_{0,act_{f,r}}$	5.8
Slow-active actuators' damping ratio	ζ	0.9
Fully-active actuators' time constant (s)	τ	0.17

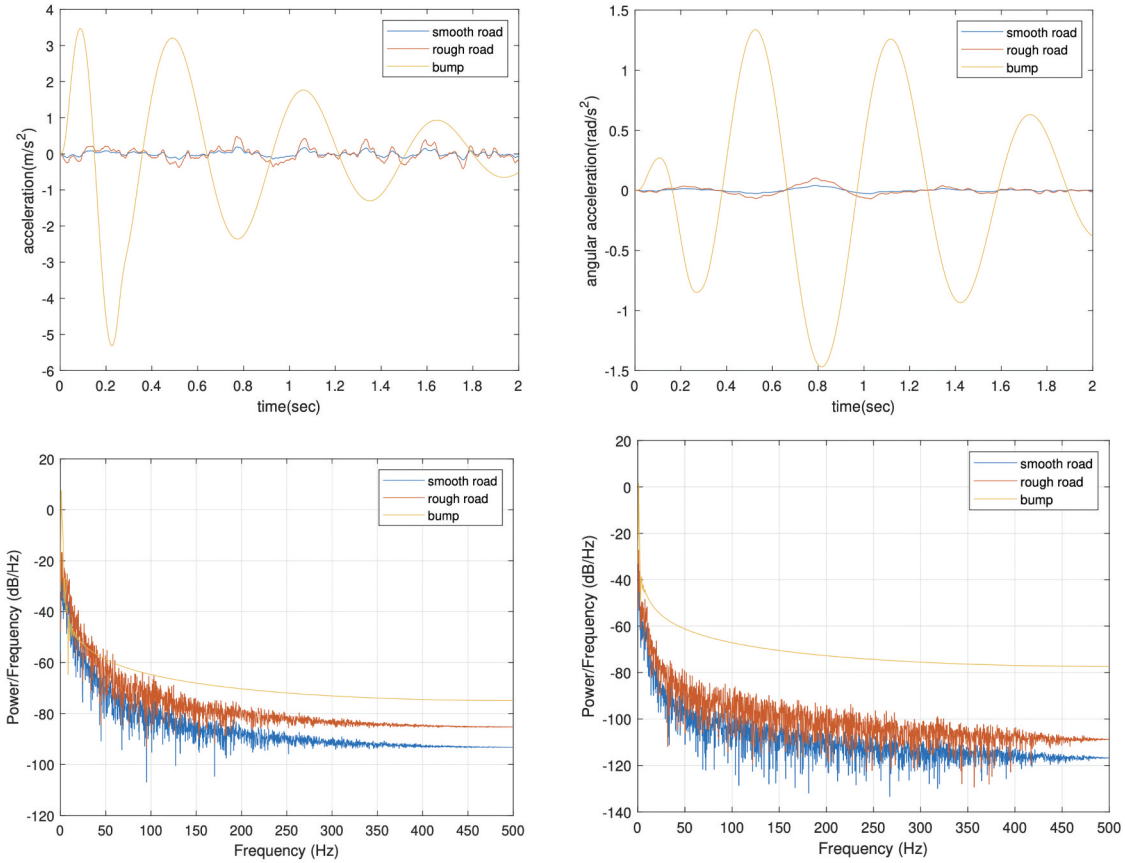

Figure 4. Passive suspension body accelerations.

Table 4. Passive suspension acceleration RMS and PSD values.

Vertical acceleration	RMS (m/s^2)	PSD Max.Amp. (dB/Hz)
Smooth	0.078	0.005
Rough	0.190	0.032
Bump	1.77	5.65
Angular Acceleration	RMS (rad/s^2)	PSD Max.Amp. (dB/Hz)
Smooth	0.013	3.05×10^{-4}
Rough	0.034	1.90×10^{-3}
Bump	0.744	1.37

PSD plots for the body linear and angular accelerations are shown in Figure 8.

Vehicle response with active suspensions to bump input and the actuator efforts are shown in Figure 9.

Tyre compressions for the front tyre with passive suspensions are shown in Figure 10. Figure 11 shows the (front) tyre compressions for smooth and rough

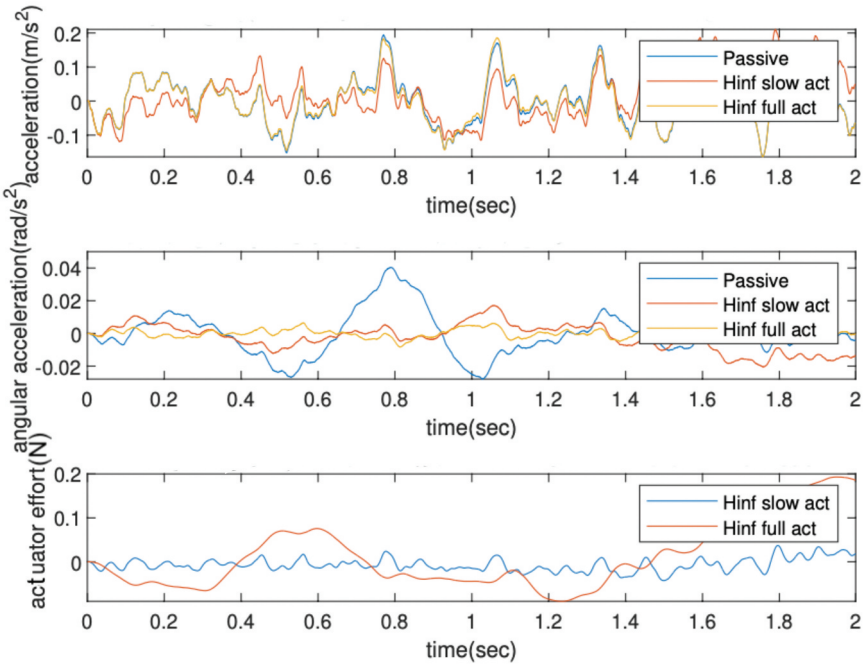

Figure 5. Suspension performance comparison for smooth road condition.

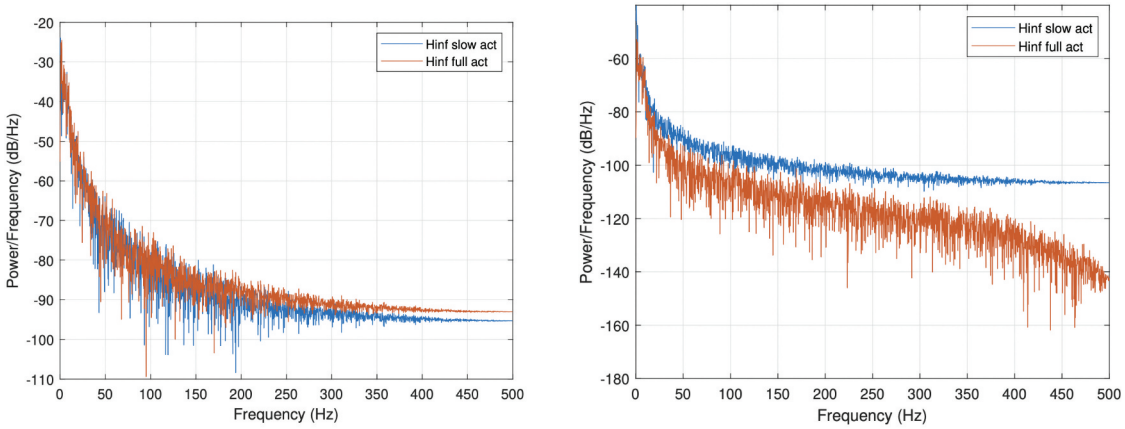

Figure 6. Active suspension body acceleration PSD for smooth road conditions.

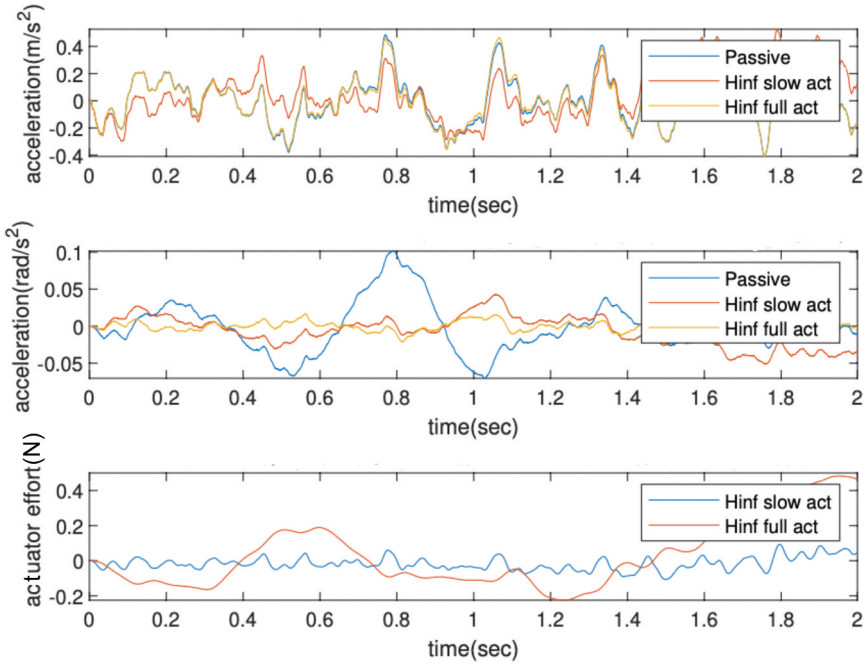

Figure 7. Suspension performance comparison for rough road condition.

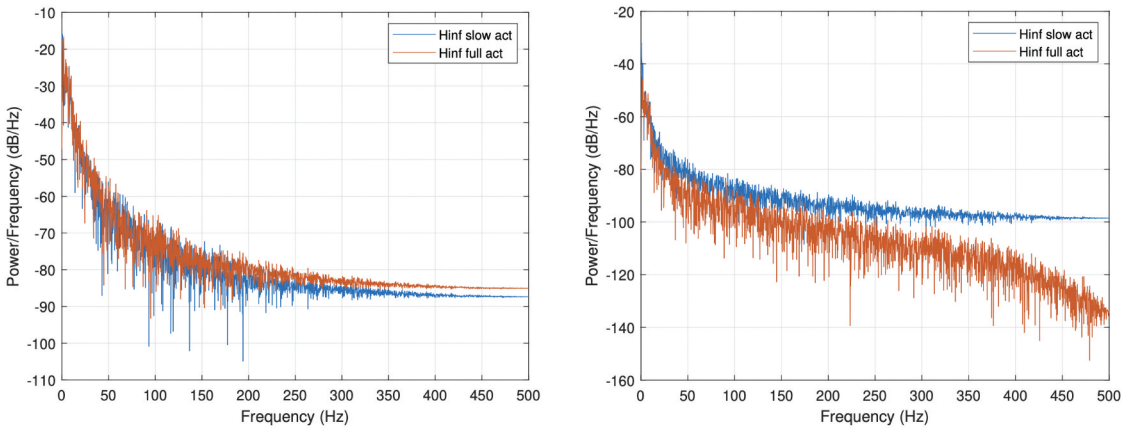

Figure 8. Active suspension body acceleration PSD for rough road conditions.

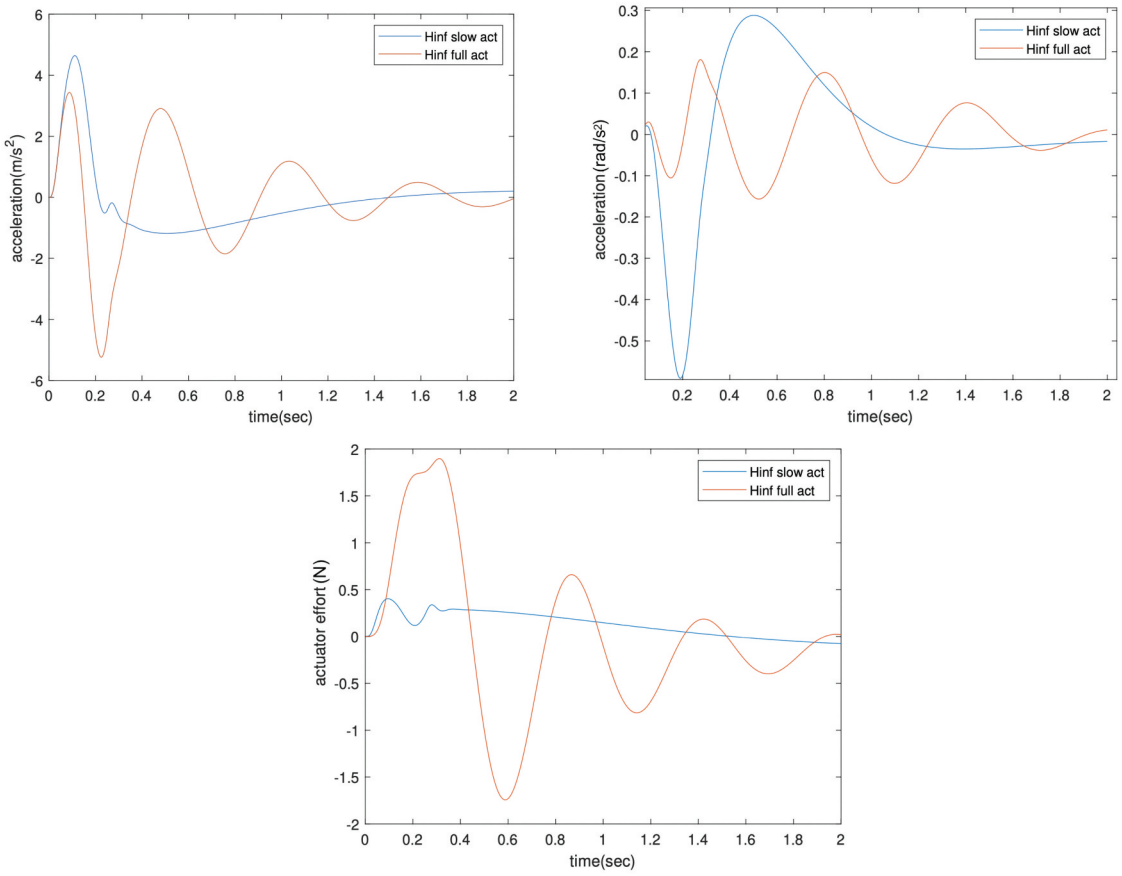

Figure 9. Active suspension performance for bump input.

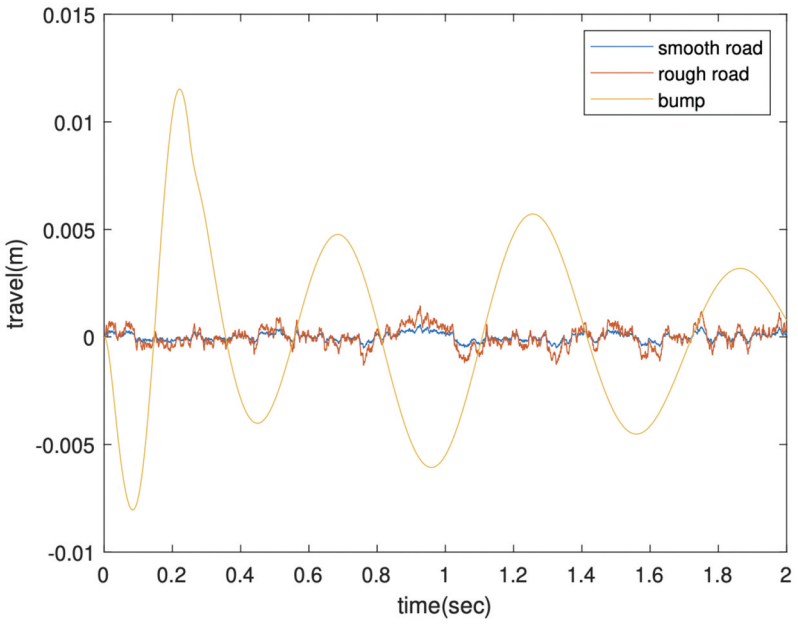

Figure 10. Passive suspension tyre compression.

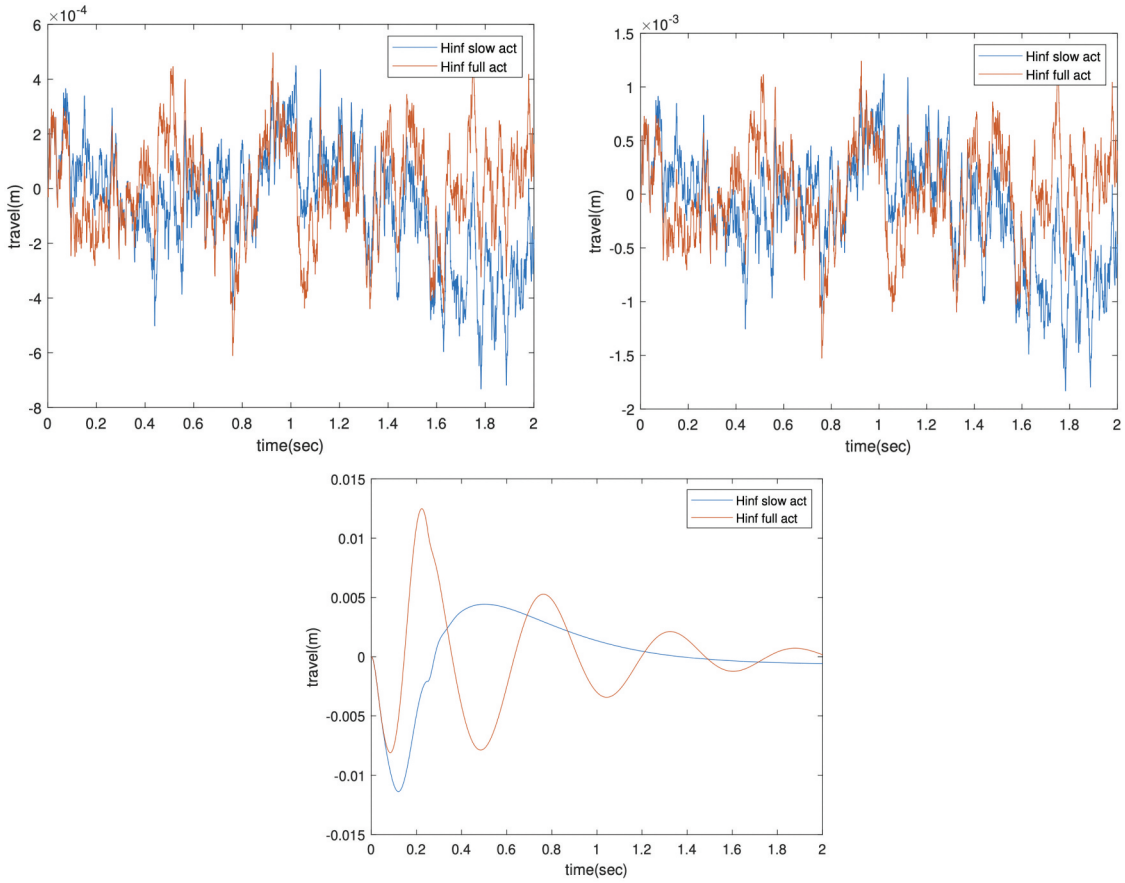

Figure 11. Active suspension (front) tyre compression comparison.

Table 5. Active suspension riding comfort improvement in relation to the passive system.

Comfort indicator/Road condition	Reduction in RMS value (%)	Reduction PSD Max.Amp. (%)
Vertical acceleration/Smooth		
Slow-active	5.49	8.88
Fully-active	13.5	22.2
Vertical acceleration/Rough		
Slow-active	2.94	19.2
Fully-active	11.2	30.9
Vertical acceleration/Bump		
Slow-active	6.94	16.7
Fully-active	10.9	17.6
Angular acceleration/Smooth		
Slow-active	37.3	68.8
Fully-active	79.8	98.3
Angular acceleration/Rough		
Slow-active	37.0	68.7
Fully-active	80.0	98.3
Angular acceleration/Bump		
Slow-active	76.5	97.3
Fully-active	89.1	99.2

road conditions on the figures above, and also for the bump input on the following figure.

4.3. Evaluation of simulation outcomes

Both active suspension systems outperform the passive suspension in simulations. The tables below summarise the results on riding comfort, on road holding and on actuator effort. Table 5 compares the performance of active systems on riding comfort relative to passive suspension.

Table 6 compares the average (front and rear) tire compression (road holding) of active suspension systems relative to the passive system.

Table 7 compares the average control effort (front and rear) of active suspension systems.

5. Conclusion

In this paper, we design and compare the performance of robust H_∞ controllers for slow and fully active

Table 6. Active suspension riding safety improvement relative to passive system.

Safety indicator/Road condition	Reduction in RMS value (%)	Reduction PSD Max.Amp. (%)
Tyre compression/Smooth		
Slow-active	−1.85	−5.81
Fully-active	7.22	26.78
Tyre compression/Rough		
Slow-active	−1.79	−5.70
Fully-active	7.27	26.8
Tyre compression/Bump		
Slow-active	11.0	53.9
Fully-active	32.0	56.1

Table 7. Active suspension average control effort RMS and PSD values.

Slow-active	RMS	PSD Max.Amp. (dB/Hz)
Smooth	0.008	4.89×10^{-5}
Rough	0.021	2.98×10^{-4}
Bump	0.159	0.054
Fully-active		
Smooth	0.038	2.15×10^{-3}
Rough	0.094	1.35×10^{-2}
Bump	0.867	1.24

electromechanical suspension systems based on a half-car model with uncertain dynamics. It is clear from Table 5 that full-active suspension system produced the best linear acceleration and angular acceleration performance, hence the best driving comfort, in relation to the passive system. Similarly, it is shown in Table 6 that full-active suspension system produced better road-holding performance relative to the passive system, whereas the slow-active suspension system has a slight reduction in performance. However, as can be noticed in Table 7, slow-active system consumes significantly less power than the fully active system. Moreover, slow-active actuators with relatively limited bandwidth are considerably cheaper than the fully active actuators. Hence, it can be concluded that, slow-active system is a better choice in active electromechanical suspension system design.

Disclosure statement

No potential conflict of interest was reported by the author(s).

Funding

The work was supported by the Marmara University Scientific Research Projects Coordination Unit [10433].

Notes on contributor

İ. Sina Kuseyri is a professor in the Mechanical Engineering Department at the Marmara University Engineering Faculty. His current research focus is on model predictive and robust control of engineering systems. Dr. Kuseyri holds a PhD in Mechanical Engineering from Boğaziçi University, İstanbul, Turkey.

ORCID

İ. Sina Kuseyri http://orcid.org/0000-0001-8134-7046

Data availability statement

The authors confirm that the data supporting the findings of this study are available within the article and/or its supplementary materials.

References

Dahlberg, T. 1978. "An Optimized Speed-Controlled Suspension of a 2-DOF Vehicle Travelling on a Randomly Profiled Road." *Journal of Sound and Vibration* 62 (4): 541–546. https://doi.org/10.1016/0022-460X(79)90462-0.

De Jager, A. 1991. "Comparison of the Two Methods for the Design of Active Suspension Systems." *Optimal Control and Applications* 12 (3): 172–188. https://doi.org/10.1002/oca.4660120305.

Doyle, J. 1978. "Guaranteed Margins for LQG Regulators." *IEEE Transactions on Automatic Control* 23 (4): 756–757. https://doi.org/10.1109/TAC.1978.1101812.

Eckert, K. 1973. "Suspension System for a Car." *Patent* 19 (11): 3741582.

El Madany, M., B. A. Bassam, and A. Fayed. 2011. "Preview Control of Slow-Active Suspension Systems." *Journal of Vibration and Control* 17 (2): 245–258. https://doi.org/10.1177/1077546310362451.

Gysen, B. L. J., J. L. G. Janssen, J. J. H. Paulides, and E. A. Lomonova. 2008. "Design Aspects of an Active Electromagnetic Suspension System for Automotive Applications." *IEEE Industry Applications Society Annual Meeting Proceedings*, Edmonton, Alberta, Canada, 1–8.

Hamersma, H., and S. Els. 2015. "A Comparison of Quarter, Half and Full Vehicle Models with Experimental Ride Comfort Data." *ASME International Design Engineering Technical Conferences and Computers and Information in Engineering Conference*, Boston, Massachusetts, USA, 1–7.

Hrovat, D. 1997. "Survey of Advanced Suspension Developments and Related Optimal Control Applications11This Paper was Not Presented at Any IFAC Meeting. This Paper was Recommended for Publication in Revised Form by Editor Karl Johan Åström.22Simple, Mostly LQ-Based Optimal Control Concepts Gave Useful Insight About Performance Potentials, Bandwidth Requirements, and Optimal Structure of Advanced Vehicle Suspensions. The Present Paper Reviews These Optimal Control Applications and Related Practical Developments."

Automatica 33 (10): 1781–1817. https://doi.org/10.1016/S0005-1098(97)00101-5.

Koch, G. P. A. 2010. "Adaptive Control of Mechatronic Vehicle Suspension Systems." *PhD Dissertation*, Technical University of Munich.

Lauwerys, C., J. Swevers, and P. Sas. 2005. "Robust Linear Control of an Active Suspension on a Quarter Car Test-Rig." *Control Engineering Practice* 13 (5): 577–586. https://doi.org/10.1016/j.conengprac.2004.04.018.

Lee, S., and W. Kim. 2010. "Active Suspension Control with Direct-Drive Tubular Linear Brushless Permanent-Magnet Motor." *IEEE Transactions on Control System Technology* 59 (4): 859–870. https://doi.org/10.1109/TCST.2009.2030413.

Li, H. 2012. "Robust Control Design for Vehicle Active Suspension Systems with Uncertainty." *PhD Dissertation*, University of Portsmouth.

Liu, H., H. Gao, P. Li, S. G. Adie, M. De Lisio, M. C. Valero, M. D. Boppart, and S. A. Boppart. 2013. "Handbook of Vehicle Suspension Control Systems." *Institution of Engineering and Technology* 1 (1): 8–19. https://doi.org/10.1142/S2339547813500027.

Michelberg, P., L. Palkovics, and J. Bokor. 1993. "Robust Design of Active Suspension System." *International Journal of Vehicle Design* 14 (2/3): 145–165. https://doi.org/10.1504/IJVD.1993.061831.

Michelberger, P., L. Palkovics, and J. Bokor. 1993. "Robust Design of Active Suspension System." *International Journal of Vehicle Design* 14 (2/3): 145–165. https://doi.org/10.1504/IJVD.1993.061831.

Pacejka, H. B., and I. J. M. Besselink. 1997. "Magic Formula Tyre Model with Transient Properties." *Vehicle System Dynamics* 27 (sup001): 234–249. https://doi.org/10.1080/00423119708969658.

Sharkawy, A. 2005. "Fuzzy and Adaptive Fuzzy Control for the automobiles' Active Suspension System." *Vehicle System Dynamics* 43 (11): 795–806. https://doi.org/10.1080/00423110500097783.

Van der Sande, T. P. J., B. L. J. Gysen, I. J. M. Besselink, J. J. H. Paulides, E. A. Lomonova, and H. Nijmeijer. 2013. "Robust Control of an Electromagnetic Active Suspension System: Simulations and Measurements." *Mechatronics* 23 (2): 204–212. https://doi.org/10.1016/j.mechatronics.2012.07.002.

Yamashita, M., K. Fujimori, K. Hayakawa, and H. Kimura. 1994. "Application of H∞ Control to Active Suspension Systems." *Automatica* 30 (11): 1717–1729. https://doi.org/10.1016/0005-1098(94)90074-4.

Zuo, L., and S. A. Nayfeh. 2003. "Low Order Continuous-Time Filters for Approximation of the ISO 2631-1 human Vibration Sensitivity Weightings." *Journal of Sound and Vibration* 265 (2): 459–465. https://doi.org/10.1016/S0022-460X(02)01567-5.